

# The microscale organization of directed hypergraphs

Quintino Francesco Lotito,<sup>1,\*</sup> Alberto Vendramini,<sup>1</sup> Alberto Montresor,<sup>1</sup> and Federico Battiston<sup>2,†</sup>

<sup>1</sup>*Department of Information Engineering and Computer Science,  
University of Trento, via Sommarive 9, 38123 Trento, Italy*

<sup>2</sup>*Department of Network and Data Science,  
Central European University, 1100 Vienna, Austria*

Many real-world complex systems are characterized by non-pairwise – higher-order – interactions among system’s units, and can be effectively modeled as hypergraphs. Directed hypergraphs distinguish between source and target sets within each hyperedge, and allow to account for the directional flow of information between nodes. Here, we provide a framework to characterize the structural organization of directed higher-order networks at their microscale. First, we extract the fingerprint of a directed hypergraph, capturing the frequency of hyperedges with a certain source and target sizes, and use this information to compute differences in higher-order connectivity patterns among real-world systems. Then, we formulate reciprocity in hypergraphs, including exact, strong, and weak definitions, to measure to which extent hyperedges are reciprocated. Finally, we extend motif analysis to identify recurring interaction patterns and extract the building blocks of directed hypergraphs. We validate our framework on empirical datasets, including Bitcoin transactions, metabolic networks, and citation data, revealing structural principles behind the organization of real-world systems.

## INTRODUCTION

Accurately modeling interactions among entities is crucial to understand the properties of many complex systems. Traditional network models focus on pairwise connections between nodes [1, 2], neglecting the complexities of systems where multiple units interact simultaneously. Such higher-order interactions are prevalent in various domains, including social networks [3, 4], folksonomies [5], ecological systems [6], chemical reactions [7] including metabolic pathways [8], and the brain [9, 10].

Hypergraphs [11] provide a framework for explicitly encoding higher-order interactions, representing them as hyperedges connecting multiple nodes simultaneously. By preserving group-based interactions, they improve our ability to understand the structures and dynamics of systems with many-body interactions [12, 13]. Recently, a variety of measures have been introduced or extended to capture the higher-order

organization of complex systems, including centrality [14, 15], community structure [16–18] and motifs [19–21]. Moreover, new models have allowed to describe systems’ evolution [22–24], and highlight the importance of higher-order interactions in shaping emergent behaviors in diffusion [25, 26], synchronization [27–29], spreading [30, 31] and evolutionary dynamics [32].

Most research has so far focused on undirected hypergraphs, which fail to capture the directional nature of many real-world interactions. For example, in a metabolic reaction, a set of reactants transforms into a set of products [8]. Similarly, in a Bitcoin transaction, multiple source wallets may transfer funds simultaneously to multiple target wallets [33]. To accurately encode such interactions, models must incorporate directionality into their representations. In this sense, directed hypergraphs enhance modeling by distinguishing between source and target sets in each hyperedge [34]. Tools to study directed hypergraphs are largely underdeveloped, with notable exceptions in areas such as null models [35], synchronization [36], overlapping patterns between two hyperedges of limited size [37], and some early proposals to define reciprocity [38, 39].

---

\* quintino.lotito@unitn.it

† battistonf@ceu.edu

In this work, we introduce measures and tools to characterize the microscale organization of real-world directed hypergraphs. First, we discuss a decomposition into fundamental interaction types: one-to-one, one-to-many, many-to-one and many-to-many. We analyze empirical data to count the occurrences of each interaction type, and use this information as a signature to compute differences in higher-order connectivity patterns. Second, we propose new simple and computationally efficient definitions for reciprocity [40] for directed hypergraphs, namely exact, strong and weak higher-order reciprocity, designed to capture different patterns of bi-directionality in empirical data. Finally, we extend motif analysis [41] to incorporate the directionality of interactions, extracting recurring higher-order and directed subgraphs. Our results suggest the existence of complex mechanisms of feedback and reinforcement in the information flow among system units, where pairwise interactions support the action of groups, and vice versa.

## RESULTS

Traditional graph models reduce directed group interactions into a collection of pairwise links, often leading to a loss of important structural information about group organization and dynamics. For instance, reducing a many-to-many interaction such as  $\text{SOURCE} = \{A, B\}$  and  $\text{TARGET} = \{D, E\}$  to a set of pairwise directed links ( $A \rightarrow D$ ,  $A \rightarrow E$ ,  $B \rightarrow D$  and  $B \rightarrow E$ ) fails to capture the collective nature of the interaction, where pairs of nodes are jointly involved in the source and target sets. Directed hypergraphs preserve group-based structure, allowing for a more faithful representation of complex interactions. In such a mathematical framework, hyperedge direction is encoded by distinguishing between source and target node sets, which are non-empty and disjoint. In particular, we distinguish four fundamental patterns of interactions encoded as directed hyperedges: one-to-one, where a single source node connects to a single target; one-to-many, where

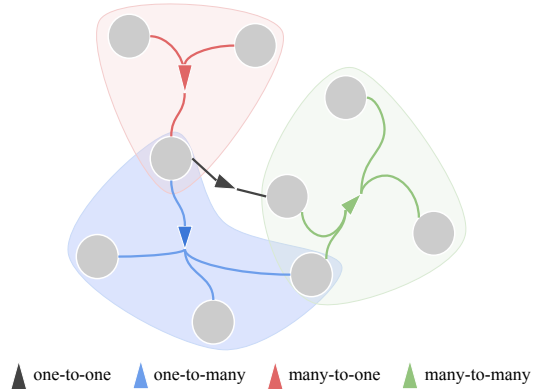


FIG. 1. **Schematic of a directed hypergraph.** Each interaction encodes a source set of units acting towards a target set of units. We distinguish four types of directed higher-order interactions: one-to-one (black), one-to-many (blue), many-to-one (red), and many-to-many (green).

one source affects multiple targets; many-to-one, where multiple sources act on a single target; and many-to-many, the most general case, where multiple sources act on multiple targets. In Figure 1, we show an example of a directed hypergraph, highlighting all distinct hyperedge patterns.

To study the microscale organization of real-world systems with directed group interactions, we collected datasets from multiple domains and mapped them into directed hypergraphs. The datasets [39] include QNA (nodes are users and forum posts are hyperedges), EMAIL (nodes are users and emails are hyperedges), BITCOIN (nodes are accounts and financial transactions are hyperedges), METABOLIC (nodes are genes and metabolic reactions are hyperedges) and CITATION (nodes are authors and hyperedges are paper citations). Detailed descriptions and summary statistics of each dataset are reported in Supplementary Note 1.

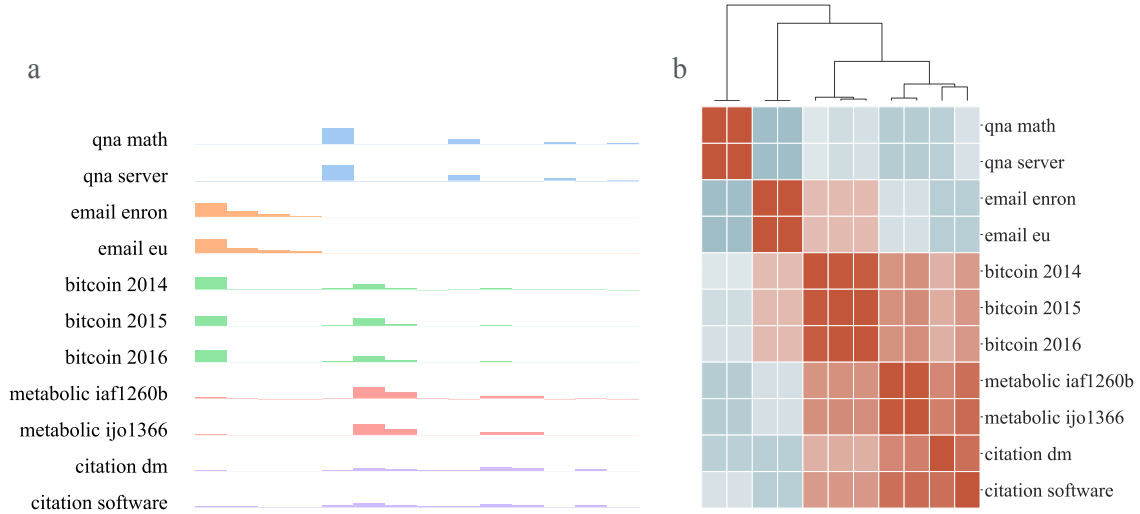


FIG. 2. **Hyperedge signature of directed hypergraphs.** a) We characterize each system with a signature hyperedge vector, encoding the abundance of a certain pattern of directed hyperedges. Systems within the same domain share the same color. b) Dendrogram resulting from agglomerative clustering applied to the correlation matrix of hyperedge signature vectors for each dataset. Correlation values are color-coded, with high positive correlations in red and high negative correlations in blue.

### Patterns of directed hyperedges

We characterize directed hypergraphs across domains by investigating the diversity in their patterns of directed hyperedges. For each dataset, we construct a *hyperedge signature vector*  $\mathbf{v}$ , which captures the distribution of hyperedges based on the sizes of their source and target sets (see Methods). Such vectors provide a fingerprint for systems based on their higher-order connectivity patterns at the microscale. Figure 2a shows the hyperedge signature vectors for each dataset, considering interactions up to size 6. To emphasize the role of higher-order interactions in the analysis, we do not consider one-to-one interactions. In the E-MAIL data we find abundance only in entries corresponding to one-to-many interactions, reflecting the typical structure of email communications. Similarly, in the QNA, many-to-one interactions are prevalent, as these systems involve multiple individuals responding to a question by a single user. In contrast, METABOLIC and CITATION datasets

show high abundances in many-to-many relationships across a variety of source and target set sizes. Finally, BITCOIN dataset exhibits more varied behavior, with abundant entries for both one-to-many and many-to-many interactions, indicating different interaction types in the network.

To further explore structural diversity across different domains, we compute pairwise correlations between hyperedge signature vectors (Pearson coefficient) and apply hierarchical agglomerative clustering on their correlation matrix. A correlation value close to 1 indicates similar hyperedge structures, 0 suggests no relationship, and  $-1$  indicates the structures are inversely related. The clustering procedure applied to the systems' correlation matrix results in a dendrogram that visually represents their hierarchical relationships, highlighting the presence of clusters of directed hypergraphs that share similar connectivity patterns. In Figure 2b, we show the correlation matrix and the clustering dendrogram. By ex-

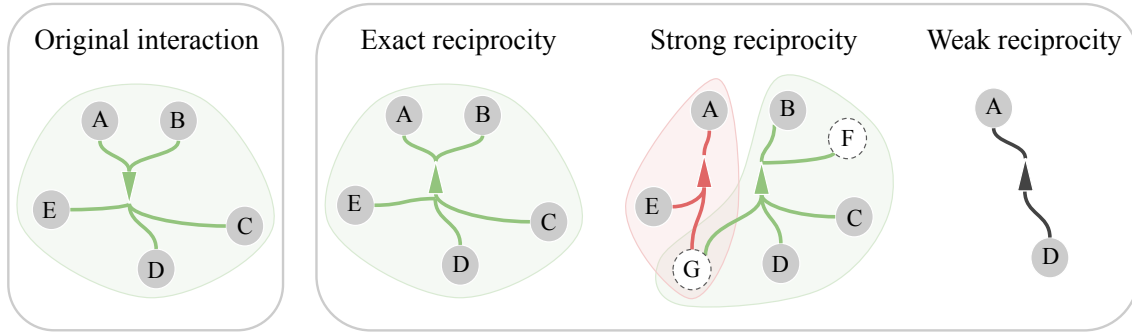


FIG. 3. **Reciprocity measures for directed hypergraphs.** For exact reciprocity, the direction of a hyperedge is fully reversed by a single hyperedge in which the source and target sets are swapped. In strong reciprocity, multiple hyperedges collectively reverse the interaction, with the source and target sets being fully reciprocated through a combination of interactions. In weak reciprocity, at least one node from the target set reciprocates an interaction with one node from the source set.

aming the correlation matrix, we observe a strong correlation within systems from the same domain, indicating highly similar abundance in hyperedge structures. In contrast, systems from different domains exhibit varying degrees of correlation. Specifically, E-MAIL and QNA datasets are inversely correlated, as they display non-overlapping and complementary connectivity patterns: E-MAIL is characterized by one-to-many interactions, whereas QNA primarily involves many-to-one relationships. The METABOLIC and CITATION datasets, which feature many-to-many interactions, are positively correlated and form a distinct cluster. Interestingly, the BITCOIN datasets also display positive correlations with the METABOLIC and CITATION cluster due to a high presence of many-to-many interaction patterns. However, they also exhibit a weaker positive correlation with the E-MAIL datasets, reflecting the presence of one-to-many interactions in BITCOIN.

### Higher-order reciprocity

Reciprocity is a fundamental property of systems with directed interactions, including social networks [42]. It traditionally refers to the tendency of the system’s units to mutu-

ally exchange directed interactions. In directed graphs, reciprocity is defined as  $r = \frac{\overleftrightarrow{L}}{L}$ , i.e., the ratio of the number of bidirectional links ( $\overleftrightarrow{L}$ ) to the total number of links ( $L$ ). This measure has been widely used to describe real-world directed networks [40, 43]. Recognizing its broad importance, recent works have extended reciprocity to hypergraphs, accounting for the complexity of having multiple nodes in both the source and target sets of hyperedges. Among the recent approaches for hypergraph reciprocity, one method decomposes hyperedges into pairwise links [38], losing information about group interactions. An alternative approach defines a more complex measure that diverges from the traditional binary definition of reciprocity at the level of single links [39]. While this can capture finer nuances, such a measure is computationally expensive and more difficult to interpret.

Here, we introduce three simple and computationally efficient measures for higher-order reciprocity in directed hypergraphs, capturing different aspects of mutual interactions:

- **Exact reciprocity** occurs when an interaction represented by a hyperedge with a source set  $h$  and a target set  $t$  is precisely mirrored by another interaction with the source and target sets reversed. For-

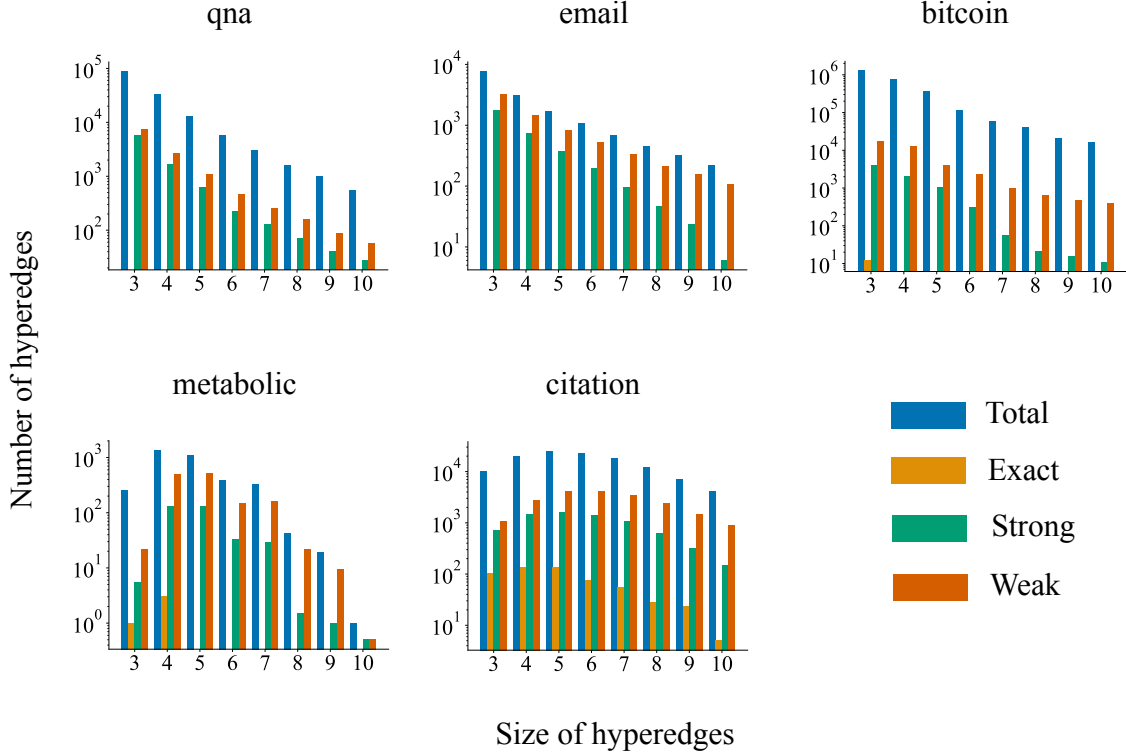


FIG. 4. **Higher-order reciprocity in real-world hypergraphs.** Number of reciprocated hyperedges for each different notion of reciprocity. In blue total hyperedges, in yellow exactly reciprocated hyperedges, in green strongly reciprocated hyperedges and in orange weakly reciprocated hyperedges. Statistics are disaggregated by hyperedge size. To simplify the plot, we grouped higher-order reciprocity of systems from the same domain.

mally, two hyperedges  $e_1 = (h_1, t_1)$  and  $e_2 = (h_2, t_2)$  are exactly reciprocated if and only if  $h_1 = t_2$  and  $t_1 = h_2$ . This is the strictest form of reciprocity.

- **Strong reciprocity** relaxes the previous requirement and allows source and target sets to be reversed through a combination of hyperedges, instead of requiring a direct reversal with a single opposite one. Formally, a hyperedge  $e = (h, t)$  is *strongly reciprocated* if there exists a set of hyperedges  $\{e_1, e_2, \dots, e_k\}$  such that the union of the target sets of  $e_1, \dots, e_k$  is a superset of the source set  $h$ , and the union of the source sets of  $e_1, \dots, e_k$  is a superset

of the target set  $t$ .

- **Weak reciprocity** represents the most relaxed form of reciprocity and requires only that at least one node from the target set of a hyperedge appears in the source set of another, and vice versa. Formally, a hyperedge  $e = (h, t)$  is *weakly reciprocated* if there exists another hyperedge  $e' = (h', t')$  such that  $h \cap t' \neq \emptyset$  and  $t \cap h' \neq \emptyset$ .

We summarize our definitions of reciprocity for directed hypergraphs in Figure 3. In Figure 4, we show statistics about the number of reciprocated hyperedges in each domain and for different definitions of reciprocity. Hyper-

edges are further disaggregated by size. Overall, every system displays a certain degree of reciprocity. In particular, weak reciprocity is widespread across domains, and the proportion of weakly reciprocated hyperedges remains relatively constant regardless of hyperedge size. Strongly reciprocated hyperedges are also common in each system, but their proportion decreases with hyperedge size at different domain-dependant rates. Conversely, exact reciprocity is rare. In particular, QNA and E-MAIL prevent exactly reciprocated hyperedges (e.g., a single e-mail cannot have more senders simultaneously). Instead, CITATION hypergraphs exhibit the highest proportion of exactly reciprocated hyperedges, observed across all hyperedge sizes. Notably, BITCOIN and QNA display the lowest levels of reciprocity across all definitions, and their degree of reciprocity is more sensitive to hyperedge size than in other systems.

### Motif analysis in directed hypergraphs

Motif analysis involves counting the frequency of patterns of interactions in connected subgraphs of a given number of nodes. This framework was first introduced by Milo et al. [41] to extract the fundamental functional units of complex systems [44]. Recently, motif analysis has been extended to hypergraphs to capture patterns of interactions with arbitrary size [19]. Here, we extend such analysis to consider also the direction of the hyperedges involved in the patterns.

First, it is interesting to study the combinatorics of the patterns of directed subhypergraphs. There is no simple closed-form formula for counting the number of possible directed higher-order motifs as a function of their order  $n$ , i.e., the number of nodes in the patterns. We can estimate the number of non-isomorphic connected directed hypergraphs in a way similar to [19]. Given a set of  $n$  nodes, the number of possible directed hyperedges is  $3^n - 2 \cdot \sum_{k=1}^n \binom{n}{k} - 1 = 3^n - 2 \cdot 2^n + 1$ . This expression counts the ways to partition the  $n$  nodes into three disjoint sets: source, target and

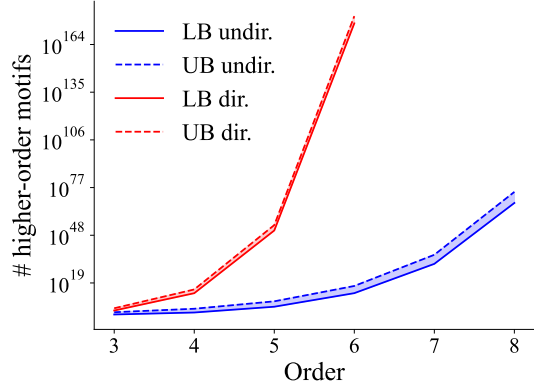


FIG. 5. **Combinatorics of directed higher-order motifs.** Upper (dashed lines) and lower (solid lines) bounds on the number of higher-order motifs as a function of their order. Blue lines refer to undirected motifs on hypergraphs, red lines refer to the directed case.

empty set. We subtract the invalid combinations with empty source or target sets. Given  $n$  nodes, we ensure connectivity by selecting a chain of  $n - 1$  hyperedges and including them in the hypergraph, leaving us with  $3^n - 2 \cdot 2^n - n + 2$  remaining possible hyperedges. For each remaining hyperedge, we decide whether to include it or not, resulting in  $2^{3^n - 2 \cdot 2^n - n + 2}$  total hypergraphs. Since we are interested in non-isomorphic hypergraphs, we divide this number by  $n!$ , the number of ways to label the vertices, providing the lower bound  $\frac{2^{3^n - 2 \cdot 2^n - n + 2}}{n!}$ . If we ignore the constraints of non-isomorphism and connectivity, we count the number of possible labeled hypergraphs. Since each of the  $3^n - 2 \cdot 2^n + 1$  possible hyperedges can either be included or excluded, the total number of labeled hypergraphs is at most  $2^{3^n - 2 \cdot 2^n + 1}$ . Figure 5 shows the upper and lower bounds on the growth of possible sub-hypergraph patterns as a function of the number of nodes (order), for both the undirected and directed cases. The estimated number of patterns grows super-exponentially, even in the undirected case. In the directed case, the growth is even faster due to the need to consider all possible subdivisions

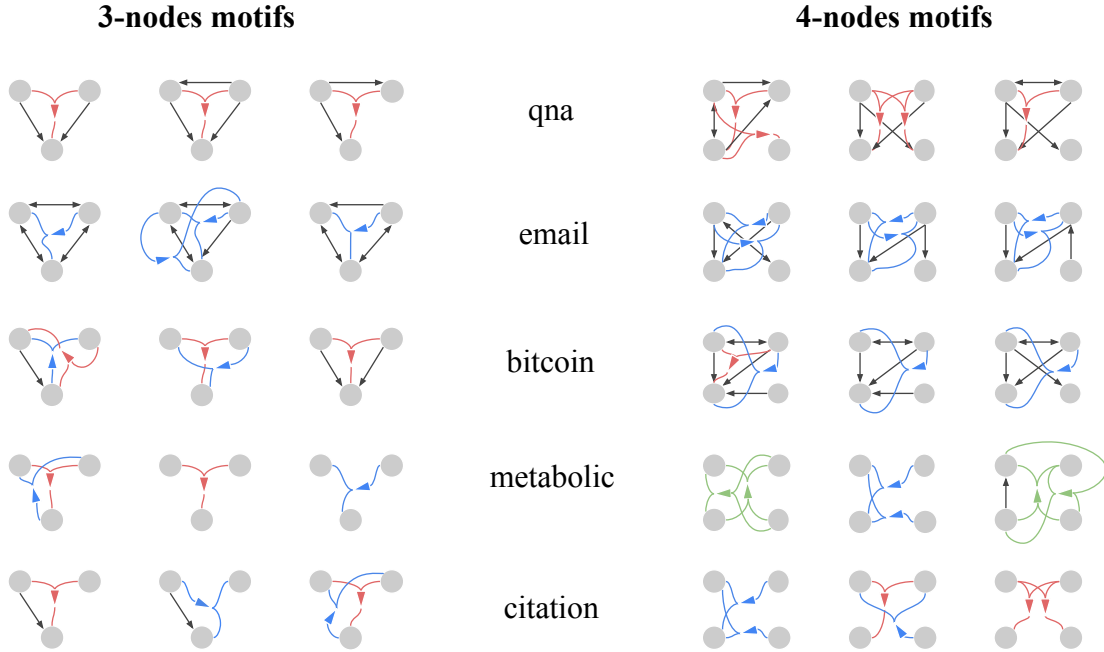


FIG. 6. **Directed higher-order motifs in real-world hypergraphs.** The three most representative directed higher-order motifs of orders three and four from each system. The color of a group interaction encodes its type: one-to-one (black), one-to-many (blue), many-to-one (red), and many-to-many (green). We group statistics of systems within the same domain.

into source and target sets.

To perform motif analysis on real-world directed hypergraphs, we propose an exact algorithm to count the frequency of all connected sub-hypergraph patterns and quantify their abundance with respect to a null model (see Methods). Given the intractability of the problem for large sub-hypergraphs, we limit our study of empirical data to patterns involving three and four nodes. Moreover, we focus on patterns that include at least one group interaction. In Figure 6, we show the most over-represented patterns of directed higher-order interactions with three and four nodes across different domains. Each domain reveals distinct motifs, characterized by different directed hyperedge types, sizes, densities and patterns of reciprocity. In terms of hyperedges types, E-MAIL and QNA involve abundant pat-

terns with only many-to-one and one-to-many interactions. Other datasets display more diverse patterns, including combinations of one-to-many, many-to-one, and many-to-many interactions (this is possible only in motifs with four nodes). Traditional one-to-one interactions are commonly part of abundant patterns in all datasets. The number of interactions in abundant sub-hypergraphs is small in the METABOLIC and CITATION domains, often involving just one or two hyperedges. In contrast, the E-MAIL, BITCOIN, and QNA domains tend to be richer in interactions. This observation is reversed when considering the average size of interactions. This relation between the number and the average size of interactions aligns with previous studies on undirected higher-order motifs [19]. A common pattern in many datasets is the coexistence of group interactions, along-

side lower-order interactions within the same set of nodes. These interactions seem to play a role in increasing the overall reciprocity of the patterns, suggesting the existence of a feedback mechanism. This is particularly evident in E-MAIL data. In addition to reciprocity, the direction of lower-order interactions in abundant patterns suggests a reinforcing mechanism, where subsets of source and target nodes interact at multiple interaction sizes. It is also likely to observe lower-order interactions among nodes that act together as a source or target of the group interaction.

## DISCUSSION

Hypergraphs extend traditional network representations by allowing hyperedges to connect multiple nodes simultaneously, enabling the encoding of group interactions ubiquitous in many relational systems. Directed hypergraphs further enhance our modelling abilities by accounting for directionality in group interactions, distinguishing between source and target sets for each hyperedge. This versatile framework can accurately model a range of diverse real-world systems and interactions, including financial transactions, email exchanges, and metabolic reactions.

In this work, we proposed new measures and tools to analyze the structural organization of directed hypergraphs at their microscale. First, we analyzed hyperedge signature vectors to identify the abundance of each hyperedge structure across datasets and identified classes of systems sharing similar higher-order connectivity patterns. Second, we introduced three distinct types of higher-order reciprocity measures: exact, strong, and weak reciprocity. Each definition offers a different perspective on how group interactions can be reciprocated, ranging from strict to more relaxed forms of reciprocal influence, and can be computed efficiently, making it suitable also for the analysis

of very large systems. We showed that all systems exhibit reciprocity in broad terms, though different domains are associated with specific patterns and sensitivity to specific reciprocity measures. Lastly, we extended the notion of motifs to directed hypergraphs, capturing recurring patterns of directed interactions. Motif analysis revealed frequent microscale structures and highlighted common organizational principles playing a role in the function and behavior of systems, such as the existence of reinforcing or feedback mechanisms among dyadic and non-dyadic interactions in groups.

Taken together, by considering the nuances related to the directionality of interactions in directed hypergraphs, our research provides a framework to understand higher-order connectivity in directed complex systems, opening up a wide range of potential applications in diverse fields such as social network analysis, biology, and finance. For instance, the study of multi-party financial transactions as directed higher-order structures may capture more complex patterns of fraudulent activity than traditional graph-based models [45]. Similarly, directed hypergraphs may enhance the accuracy of existing frameworks in identifying and predicting important genes based on genomic expression relations [46]. As scalability is a pressing issue in hypergraph algorithms, future work may explore advanced techniques for detecting motifs in large-scale directed hypergraphs, including sampling methods [47], to expand our analysis beyond patterns of four nodes. Another interesting venue for further studies is related to the study of reciprocity in weighted or time-evolving hypergraphs, where interactions are associated with different intensities or specific moments in time. All in all, our work reveals new structural principles behind the organization of real-world systems, shedding light on the complex interplay between structural patterns and functionality in directed complex systems.



## METHODS

### Hyperedge signature vector construction

For each dataset, we construct a *hyperedge signature vector*  $\mathbf{v}$ , where each element represents the count of hyperedges with a specific combination of source set size  $s$  and target set size  $t$  in the hypergraph. The vector  $\mathbf{v}$  captures the distribution of hyperedges based on the sizes of their source and target sets, providing a profile of the hypergraph structure.

Formally, we define the vector  $\mathbf{v}$  as follows:

$$\mathbf{v} = (v_{1,2}, \dots, v_{1,K-1}, v_{2,1}, \dots, v_{2,K-2}, \dots, v_{K-1,1})$$

where  $K$  represents the maximum hyperedge size considered, and each  $v_{h,t}$  counts the number of hyperedges with a specific source size  $h$  and target size  $t$ .

### Algorithms for measuring reciprocity in directed hypergraphs

Below, we outline our proposed algorithms for efficiently measuring reciprocity in directed hypergraphs.

- **Exact reciprocity.** Each hyperedge  $e = (s, t)$  is stored in a hash-based dictionary, and for each hyperedge, we search for a reverse hyperedge  $e' = (t, s)$ . Since each lookup takes constant time, the overall complexity is  $O(m)$ , where  $m$  is the number of hyperedges.
- **Strong reciprocity.** For each hyperedge  $e = (s, t)$ , we maintain a reachability dictionary that tracks which nodes in the target set  $t$  can reach other nodes via multiple hyperedges. We then check whether the source set  $s$  is fully covered by the accumulated reachable nodes from the target set  $t$ . This involves iterating over each hyperedge, for each target node, accumulating the reachable nodes and then checking if the source set is a subset of this accumulated set. Computing the union of reachable nodes is  $O(s \cdot t)$ , where  $s$  is the maximum size of source sets and  $t$  is the maximum size of target sets. This operation is repeated for all hyperedges, leading to a total complexity of  $O(m \cdot s \cdot t)$ .
- **Weak reciprocity.** First, we construct a dictionary to store all directed node pairs between the source and target sets of each hyperedge. Then, for each hyperedge, we check whether any of its target nodes are linked back to the source nodes via reverse connections in the dictionary. The computational complexity is dominated by the first operation, which is  $O(m \cdot s \cdot t)$ , where  $s$  is the maximum size of the source sets and  $t$  is the maximum size of the target sets across all hyperedges.

In practice, executing these algorithms on the real-world datasets used in our experiments requires only a few minutes for all datasets combined, demonstrating the computational efficiency of the proposed methods.

### Algorithms for motif analysis in directed hypergraphs

In order to design efficient algorithms for mining directed higher-order motifs, we extend prior ideas developed for the same problem in undirected hypergraphs [47]. Our algorithms are efficient

enough to count motifs of size 3 and 4 in datasets of reasonable size (comparable to those used in our experiments). However, scaling to larger datasets and motifs of larger size would require more sophisticated approaches, such as sampling algorithms [47], which we leave for future work. Further details on the execution times of the algorithms for mining motifs of orders 3 and 4 can be found in Supplementary Notes 2.

The algorithm for mining motifs (involving at least one group interaction) of order 3 begins by iterating through each hyperedge in the hypergraph that contains exactly three vertices. For each such hyperedge, it identifies all possible subsets of vertices and checks whether one or more subsets form valid directed hyperedges in the hypergraph. Valid subsets, along with the original hyperedge, define the motif structure involving those three vertices. To ensure consistency in motif identification, the algorithm generates a canonical form of the motif by lexicographical ordering its vertices and edges, which can be computed by sorting the  $n!$  possible relabels. This canonical representation allows motifs with the same structural pattern to be compared and counted, even if they differ in their vertex labels. Each canonical form of motifs is stored in a frequency hash map. If the motif has not been encountered before, it is added to the map; if it has, its frequency count is incremented. In the end, the algorithm outputs a distribution of the various motif structures of order 3. This algorithm operates in linear time with respect to the number of hyperedges of order 3. Specifically, its computational complexity is  $O(m_3)$ , where  $m_3$  is the number of hyperedges involving exactly three vertices. Each motif construction and comparison is performed in constant time due to the fixed size of the motifs. For more details, refer to the pseudocode in Supplementary Note 2.

The algorithm for mining motifs of order 4 follows a similar approach. First, it iterates over all hyperedges of size 4, counting the motifs involving exactly these 4 nodes. Unlike the previous algorithm, it then iterates over all hyperedges of size 3, performing an additional neighborhood exploration step to identify the fourth node involved in the motif. Each neighboring node is considered during this process. Once the 4 nodes are identified, the algorithm constructs the motif as before. The pseudocode for this algorithm is provided in Supplementary Note 2.

### Statistical significance of motifs

To distinguish meaningful, non-random interaction patterns from those that may occur by chance, we use a configuration model as a null model to evaluate the statistical significance of the interaction patterns after computing their frequency in our directed hypergraphs. The configuration model generates randomized versions of the original hypergraph while preserving key properties, such as the in-degree and out-degree sequences, as well as the source and target sizes of the hyperedges [35]. By comparing the observed frequencies with those found in the randomized networks, we can identify significantly over-represented motifs. In particular, each motif is associated with the abundance score  $\Delta_i$  relative to random networks proposed in [44],

$$\Delta_i = \frac{N_{\text{real}_i} - \langle N_{\text{rand}_i} \rangle}{N_{\text{real}_i} + \langle N_{\text{rand}_i} \rangle + \epsilon} \quad (1)$$

Following [19, 44], we set  $\epsilon = 4$ . We sample  $N = 10$  times from the configuration model.

### CODE AVAILABILITY

Available as part of Hypergraphx (HGX) [48].

## DATA AVAILABILITY

Data [39] is publicly available and also easily accessible through HGX [48].

## ACKNOWLEDGEMENTS

F.B. acknowledges support from the Air Force Office of Scientific Research under award number FA8655-22-1-7025. A.M. acknowledges support from the European Union through Horizon Europe CLOUDSTARS project (101086248).

- 
- [1] S. Boccaletti, V. Latora, Y. Moreno, M. Chavez, and D.-U. Hwang, Complex networks: Structure and dynamics, *Physics Reports* **424**, 175 (2006).
  - [2] G. Cimini, T. Squartini, F. Saracco, D. Garlaschelli, A. Gabrielli, and G. Caldarelli, The statistical physics of real-world networks, *Nature Reviews Physics* **1**, 58 (2019).
  - [3] A. Patania, G. Petri, and F. Vaccarino, The shape of collaborations, *EPJ Data Science* **6**, 1 (2017).
  - [4] G. Cencetti, F. Battiston, B. Lepri, and M. Karsai, Temporal properties of higher-order interactions in social networks, *Scientific Reports* **11**, 1 (2021).
  - [5] G. Ghoshal, V. Zlatić, and G. Caldarelli, Random hypergraphs and their applications, *Physical Review E* **79**, 066118 (2009).
  - [6] J. Grilli, G. Barabás, M. J. Michalska-Smith, and S. Allesina, Higher-order interactions stabilize dynamics in competitive network models, *Nature* **548**, 210 (2017).
  - [7] J. Jost and R. Mulas, Hypergraph laplace operators for chemical reaction networks, *Advances in Mathematics* **351**, 870 (2019).
  - [8] P. Traversa, G. Ferraz de Arruda, A. Vazquez, and Y. Moreno, Robustness and complexity of directed and weighted metabolic hypergraphs, *Entropy* **25**, 1537 (2023).
  - [9] G. Petri, P. Expert, F. Turkheimer, R. Carhart-Harris, D. Nutt, P. J. Hellyer, and F. Vaccarino, Homological scaffolds of brain functional networks, *Journal of The Royal Society Interface* **11**, 20140873 (2014).
  - [10] A. Santoro, F. Battiston, M. Lucas, G. Petri, and E. Amico, Higher-order connectomics of human brain function reveals local topological signatures of task decoding, individual identification, and behavior, *bioRxiv*, 2023 (2023).
  - [11] C. Berge, *Graphs and hypergraphs* (North-Holland Pub. Co., 1973).
  - [12] F. Battiston, G. Cencetti, I. Iacopini, V. Latora, M. Lucas, A. Patania, J.-G. Young, and G. Petri, Networks beyond pairwise interactions: structure and dynamics, *Physics Reports* **874**, 1 (2020).
  - [13] F. Battiston, E. Amico, A. Barrat, G. Bianconi, G. Ferraz de Arruda, B. Franceschiello, I. Iacopini, S. Kéfi, V. Latora, Y. Moreno, *et al.*, The physics of higher-order interactions in complex systems, *Nature Physics* **17**, 1093 (2021).
  - [14] A. R. Benson, Three hypergraph eigenvector centralities, *SIAM Journal on Mathematics of Data Science* **1**, 293 (2019).
  - [15] F. Tudisco and D. J. Higham, Node and edge nonlinear eigenvector centrality for hypergraphs, *Communications Physics* **4**, 1 (2021).
  - [16] A. Eriksson, D. Edler, A. Rojas, M. de Domenico, and M. Rosvall, How choosing random-walk model and network representation matters for flow-based community detection in hypergraphs, *Communications Physics* **4**, 1 (2021).
  - [17] M. Contisciani, F. Battiston, and C. De Bacco, Inference of hyperedges and overlapping communities in hypergraphs, *Nature communications* **13**, 1 (2022).
  - [18] N. Ruggeri, M. Contisciani, F. Battiston, and C. De Bacco, Community detection in large

- hypergraphs, *Science Advances* **9**, eadg9159 (2023).
- [19] Q. F. Lotito, F. Musciotto, A. Montresor, and F. Battiston, Higher-order motif analysis in hypergraphs, *Communications Physics* **5**, 79 (2022).
- [20] G. Lee, J. Ko, and K. Shin, Hypergraph motifs: concepts, algorithms, and discoveries, *Proceedings of the VLDB Endowment* **13**, 2256 (2020).
- [21] B. Arregui-García, A. Longa, Q. F. Lotito, S. Meloni, and G. Cencetti, Patterns in temporal networks with higher-order egocentric structures, arXiv preprint arXiv:2402.03866 (2024).
- [22] G. Petri and A. Barrat, Simplicial activity driven model, *Physical review letters* **121**, 228301 (2018).
- [23] L. Di Gaetano, F. Battiston, and M. Starnini, Percolation and topological properties of temporal higher-order networks, *Physical Review Letters* **132**, 037401 (2024).
- [24] L. Gallo, L. Lacasa, V. Latora, and F. Battiston, Higher-order correlations reveal complex memory in temporal hypergraphs, *Nature Communications* **15**, 4754 (2024).
- [25] M. T. Schaub, A. R. Benson, P. Horn, G. Lippner, and A. Jadbabaie, Random walks on simplicial complexes and the normalized hodge 1-laplacian, *SIAM Review* **62**, 353 (2020).
- [26] T. Carletti, F. Battiston, G. Cencetti, and D. Fanelli, Random walks on hypergraphs, *Physical Review E* **101**, 022308 (2020).
- [27] M. Lucas, G. Cencetti, and F. Battiston, Multiorder laplacian for synchronization in higher-order networks, *Physical Review Research* **2**, 033410 (2020).
- [28] L. V. Gambuzza, F. Di Patti, L. Gallo, S. Lepri, M. Romance, R. Criado, M. Frasca, V. Latora, and S. Boccaletti, Stability of synchronization in simplicial complexes, *Nature Communications* **12**, 1 (2021).
- [29] Y. Zhang, M. Lucas, and F. Battiston, Higher-order interactions shape collective dynamics differently in hypergraphs and simplicial complexes, *Nature Communications* **14**, 1605 (2023).
- [30] I. Iacopini, G. Petri, A. Barrat, and V. Latora, Simplicial models of social contagion, *Nature Communications* **10**, 1 (2019).
- [31] S. Chowdhary, A. Kumar, G. Cencetti, I. Iacopini, and F. Battiston, Simplicial contagion in temporal higher-order networks, *Journal of Physics: Complexity* **2**, 035019 (2021).
- [32] A. Civilini, O. Sadekar, F. Battiston, J. Gómez-Gardeñes, and V. Latora, Explosive cooperation in social dilemmas on higher-order networks, *Physical Review Letters* **132**, 167401 (2024).
- [33] S. Ranshous, C. A. Joslyn, S. Kreyling, K. Nowak, N. F. Samatova, C. L. West, and S. Winters, Exchange pattern mining in the bitcoin transaction directed hypergraph, in *Financial Cryptography and Data Security: FC 2017 International Workshops, WAHC, BITCOIN, VOTING, WTSC, and TA, Sliema, Malta, April 7, 2017, Revised Selected Papers 21* (Springer, 2017) pp. 248–263.
- [34] G. Gallo, G. Longo, S. Pallottino, and S. Nguyen, Directed hypergraphs and applications, *Discrete Applied Mathematics* **42**, 177 (1993).
- [35] G. Preti, A. Fazzino, G. Petri, and G. De Francisci Morales, Higher-order null models as a lens for social systems, *Physical Review X* **14**, 031032 (2024).
- [36] L. Gallo, R. Muolo, L. V. Gambuzza, V. Latora, M. Frasca, and T. Carletti, Synchronization induced by directed higher-order interactions, *Communications Physics* **5**, 263 (2022).
- [37] H. Moon, H. Kim, S. Kim, and K. Shin, Four-set hypergraphlets for characterization of directed hypergraphs, arXiv preprint arXiv:2311.14289 (2023).
- [38] N. Pearcy, J. J. Crofts, and N. Chuzhanova, Hypergraph models of metabolism, *International Journal of Biological, Veterinary, Agricultural and Food Engineering* **8**, 752 (2014).
- [39] S. Kim, M. Choe, J. Yoo, and K. Shin, Reciprocity in directed hypergraphs: measures, findings, and generators, *Data Mining and Knowledge Discovery* **37**, 2330 (2023).
- [40] D. Garlaschelli and M. I. Loffredo, Patterns of link reciprocity in directed networks, *Physical review letters* **93**, 268701 (2004).
- [41] R. Milo, S. Shen-Orr, S. Itzkovitz, N. Kashtan, D. Chklovskii, and U. Alon, Network motifs: Simple building blocks of complex networks, *Science* **298**, 824 (2002).
- [42] S. Wasserman, K. Faust, *et al.*, *Social network analysis: Methods and applications* (Cambridge university press, 1994).
- [43] M. E. J. Newman, S. Forrest, and J. Balthrop, Email networks and the spread of computer viruses, *Phys. Rev. E* **66**, 035101 (2002).
- [44] R. Milo, S. Itzkovitz, N. Kashtan, R. Levitt, S. Shen-Orr, I. Ayzenshtat, M. Sheffer, and

- U. Alon, Superfamilies of evolved and designed networks, *Science* **303**, 1538 (2004).
- [45] L. Akoglu, H. Tong, and D. Koutra, Graph based anomaly detection and description: a survey, *Data mining and knowledge discovery* **29**, 626 (2015).
- [46] S. Feng, E. Heath, B. Jefferson, C. Joslyn, H. Kvinge, H. D. Mitchell, B. Praggastis, A. J. Eisfeld, A. C. Sims, L. B. Thackray, *et al.*, Hypergraph models of biological networks to identify genes critical to pathogenic viral response, *BMC bioinformatics* **22**, 287 (2021).
- [47] Q. F. Lotito, F. Musciotto, F. Battiston, and A. Montresor, Exact and sampling methods for mining higher-order motifs in large hypergraphs, *Computing* **106**, 475 (2024).
- [48] Q. F. Lotito, M. Contisciani, C. De Bacco, L. Di Gaetano, L. Gallo, A. Montresor, F. Musciotto, N. Ruggeri, and F. Battiston, Hypergraphx: a library for higher-order network analysis, *Journal of Complex Networks* **11**, cnad019 (2023).
- [49] P. Chodrow and A. Mellor, Annotated hypergraphs: models and applications, *Applied network science* **5**, 9 (2020).
- [50] L. Jure, Snap datasets: Stanford large network dataset collection, Retrieved December 2021 from <http://snap.stanford.edu/data> (2014).
- [51] J. Wu, J. Liu, W. Chen, H. Huang, Z. Zheng, and Y. Zhang, Detecting mixing services via mining bitcoin transaction network with hybrid motifs, *IEEE Transactions on Systems, Man, and Cybernetics: Systems* **52**, 2237 (2021).
- [52] N. Yadati, V. Nitin, M. Nimishakavi, P. Yadav, A. Louis, and P. Talukdar, Nhp: Neural hypergraph link prediction, in *Proceedings of the 29th ACM international conference on information & knowledge management* (2020) pp. 1705–1714.
- [53] A. Sinha, Z. Shen, Y. Song, H. Ma, D. Eide, B.-J. Hsu, and K. Wang, An overview of microsoft academic service (mas) and applications, in *Proceedings of the 24th international conference on world wide web* (2015) pp. 243–246.
- [54] N. Yadati, T. Gao, S. Asoodeh, P. Talukdar, and A. Louis, Graph neural networks for soft semi-supervised learning on hypergraphs, in *Pacific-Asia Conference on Knowledge Discovery and Data Mining* (Springer, 2021) pp. 447–458.
-

Dataset	$ V $	$ E $	$\overline{ S_i }$	$\overline{ T_i }$
bitcoin-2014	1 697 625	1 437 082	1.478	1.697
bitcoin-2015	1 961 886	1 449 827	1.568	1.744
bitcoin-2016	2 009 978	1 451 135	1.495	1.715
metabolic-iaf1260b	1 668	2 083	1.998	2.267
metabolic-iJO1366	1 805	2 251	2.026	2.272
email-enron	110	1 484	1.000	2.354
email-eu	986	35 772	1.000	2.368
citation-dm	27 164	73 113	3.253	3.038
citation-software	16 555	53 177	2.927	2.717
qna-math	34 812	93 731	1.779	1.000
qna-server	172 330	272 116	1.747	1.000

TABLE S1. Summary statistics of the datasets used in our experiments.

## SUPPLEMENTARY INFORMATION

### Supplementary Note 1. Datasets

This section provides detailed descriptions of the datasets used in our experiments. The datasets are originally collected in [39] and represent a diverse range of real-world systems with directed higher-order interactions. Summary statistics of the datasets used in our experiments are reported in Table S1.

- **Question answering data.** We use two QNA datasets: Math-overflow and Server-fault, both sourced from Stack Exchange logs. A hyperedge  $e_i = (S_i, T_i)$  indicates a question posted by the user in the target set  $T_i$  and answered by the users in the source set  $S_i$ . Each hyperedge has a unit target set, i.e.,  $|T_i| = 1, \forall i = \{1, \dots, |E|\}$ .
- **Email data.** We use two email datasets: email-enron [49] and email-eu [50]. A hyperedge  $e_i = (S_i, T_i)$  represents an email where the sender is the source set  $S_i$ , and the receivers (including cc-ed users) form the target set  $T_i$ . Each hyperedge has a unit source set, i.e.,  $|S_i| = 1, \forall i = \{1, \dots, |E|\}$ .
- **Bitcoin transactions data.** We use three bitcoin transaction datasets: bitcoin-2014, bitcoin-2015, and bitcoin-2016 [51]. They contain the first 1 500 000 transactions in 11/2014, 06/2015, and 01/2016 respectively. A hyperedge  $e_i = (S_i, T_i)$  corresponds to a transaction where the accounts from which the coins are sent form the source set  $S_i$ , and the accounts receiving the coins make up the target set  $T_i$ .
- **Metabolic data.** We use two metabolic datasets: iAF1260b and iJO1366 [52]. Nodes are the genes and hyperedges are metabolic reactions. A hyperedge  $e_i = (S_i, T_i)$  indicates that the reaction among genes in the source set  $S_i$  results in genes in the target set  $T_i$ .
- **Citation data.** We use two citation datasets: citation-data mining and citation-software [53, 54]. A hyperedge  $e_i = (S_i, T_i)$  represents a citation from a paper co-authored by the authors in the source set  $S_i$  to a paper co-authored by the authors in the target set  $T_i$ . Papers with more than 10 authors are filtered out.

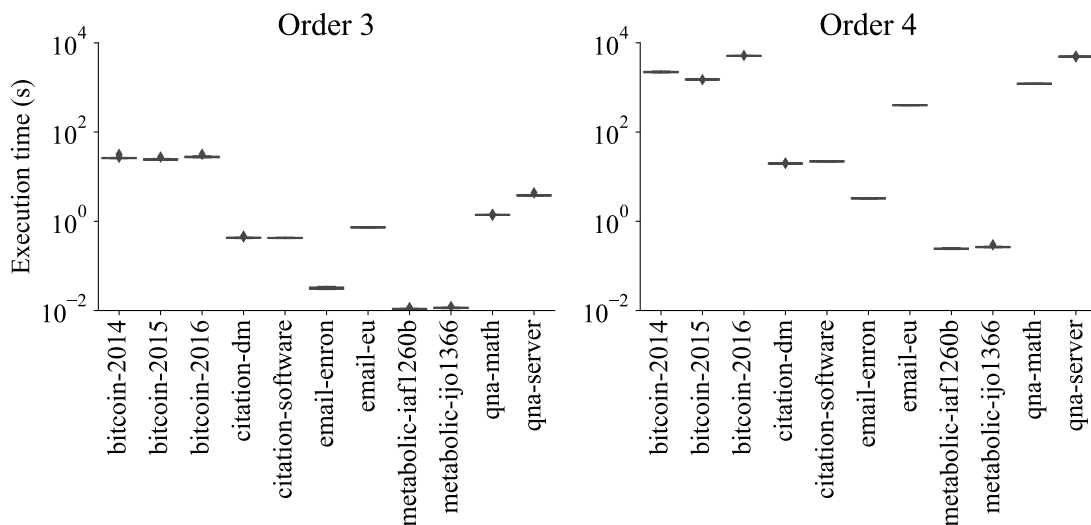


FIG. S1. Execution times in seconds of the algorithms for mining motifs of order 3 and 4 across datasets. We consider 10 trials for each dataset.

### Supplementary Note 2. Algorithms for motif analysis in directed hypergraphs

This section provides further details on the algorithms for motif analysis in directed hypergraphs. In Fig. S1, we show the execution times of our algorithms for motifs of order 3 and 4 across various datasets, highlighting the increase in time when moving from order 3 to order 4. More complex approaches will be needed to scale the analysis to larger motifs and larger dataset sizes. In Algorithm 1 and Algorithm 2, we present detailed pseudocode for the algorithms designed to count directed higher-order motifs of sizes 3 and 4, respectively.

---

**Algorithm 1** Motifs of order 3
 

---

**Input:** A directed hypergraph  $\mathcal{H} = (V, E)$

**Output:** distribution of the frequency of the motifs of order 3

```

1: Let  $M$  be the motifs frequency hash map
2: Let  $U$  be the isomorphism class hash map
3: for each hyperedge  $e$  of order 3 in  $E$  do
4:    $V^* \leftarrow$  vertices of  $e$ 
5:    $motif \leftarrow \emptyset$ 
6:   for each  $e^* \in \mathcal{P}(V^*)$  do
7:     if  $e^* \in E$  then
8:        $motif \leftarrow motif \cup e^*$ 
9:     end if
10:  end for each
11:   $C_m \leftarrow$  lexicographically minimum canonic relabel of  $motif$ 
12:  if  $C_m \notin M$  then
13:     $M[C_m] \leftarrow 0$ 
14:  end if
15:   $M[C_m] + = 1$ 
16:  Set vertices of  $motif$  as visited
17: end for each

```

---



---

**Algorithm 2** Motifs of order 4
 

---

**Input:** A directed hypergraph  $H = (V, E)$

**Output:** distribution of the frequency of the motifs of order 4

```

1: Let  $M$  be the motifs frequency hash map
2: Let  $s$  be the isomorphism class hash map
3: for each hyperedge  $e$  of order 4 in  $E$  do
4:    $V^* \leftarrow$  vertices of  $e$ 
5:    $motif \leftarrow \emptyset$ 
6:   for each  $e^* \in \mathcal{P}(V^*)$  do
7:     if  $e^* \in E$  then
8:        $motif \leftarrow motif \cup e^*$ 
9:     end if
10:  end for each
11:   $C_m \leftarrow$  lexicographically minimum canonic relabel of  $motif$ 
12:  if  $C_m \notin M$  then
13:     $M[C_m] \leftarrow 0$ 
14:  end if
15:   $M[C_m] + = 1$ 
16:  Set vertices of  $motif$  as visited
17: end for each
18:  $\mathcal{H} \leftarrow$  Discard all hyperedges of order 4 from  $\mathcal{H}$ 
19: for each hyperedge  $e$  of order 3 in  $E$  do
20:   Let  $\mathcal{Z}$  be the set of hyperedges adjacent to  $e$ 
21:   for each hyperedge  $\zeta$  in  $\mathcal{Z}$  do
22:     if  $|\zeta \cup e| = 4$  and  $\zeta \cup e$  not already visited then
23:        $V^* \leftarrow$  vertices of  $\zeta \cup e$ 
24:        $motif \leftarrow \emptyset$ 
25:       for each  $e^* \in \mathcal{P}(V^*)$  do
26:         if  $e^* \in E$  then
27:            $motif \leftarrow motif \cup e^*$ 
28:         end if
29:       end for each
30:        $C_m \leftarrow$  lexicographically minimum canonic relabel of  $motif$ 
31:       if  $C_m \notin M$  then
32:          $M[C_m] \leftarrow 0$ 
33:       end if
34:        $M[C_m] + = 1$ 
35:       Set vertices of  $motif$  as visited
36:     end if
37:   end for each
38: end for each

```

---